Silica formation in diatoms: the function of long-chain polyamines and silaffins

Manfred Sumper and Nils Kröger*

Lehrstuhl Biochemie I, Universität Regensburg, D-93053 Regensburg, Germany.
E-mail: manfred.sumper@vkl.uni-regensburg.de; E-mail: nils.kroeger@vkl.uni-regensburg.de;
Fax: +49 941 943-2936; Tel: +49 941 943-2833

The stunning silica structures formed by diatoms are among the most remarkable examples of biological nanofabrication. In recent years, insight into the molecules and mechanism that allow diatoms to perform silica morphogenesis under ambient conditions has been gained.

Introduction

The formation of inorganic minerals under the control of an organism (biomineralization) is a widespread phenomenon in nature. Silica is the second most abundant biomineral being exceeded only by biogenic $CaCO_3$.[1] Many landplants (*e.g.* rice, cereals, cucumber) deposit silica in significant amounts to reinforce their tissues[2] and as a systemic response to pathogen attack.[3] Furthermore, there is evidence that silica is required in animals including mammals for proper development of cartilage and bone.[4,5] Silica biomineralization on earth, however, is dominated by simple aquatic life forms including unicellular organisms like diatoms, radiolaria and synurophytes as well as multicellular sponges.[1] These organisms produce silica-based exo- and endo-skeletons that account for the majority of their body mass and, most notably in diatoms, exhibit intricate cell wall patterns in the nano- to micro-meter range (biosilica nanopatterns) (Fig. 1). Since the biosilica nanopatterns are precisely reproduced in a species-specific manner in each generation, a genetic control of this biomineralization process is obvious which has been regarded as a paradigm for controlled production of nanostructured silica. Therefore, understanding the mechanism of silica nanofabrication by diatoms may inspire synthetic routes to produce novel silica-based materials under mild reaction conditions.[6,7] Diatom biosilica is mainly composed of amorphous, hydrated SiO_2 (silica) containing a small proportion of organic
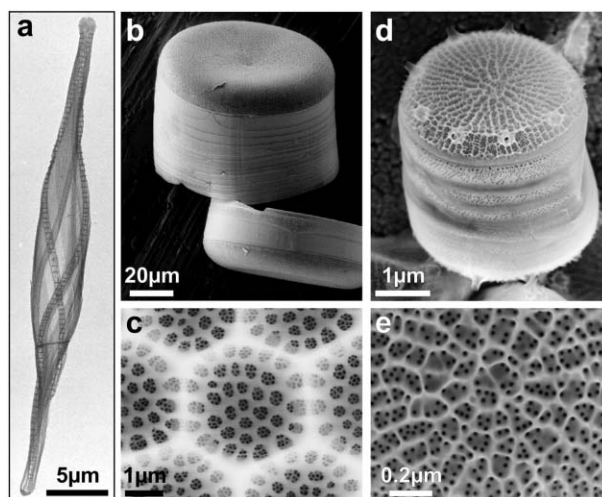

Fig. 1 Structures of diatom cell walls. Electron microscopy images of isolated cell walls from different diatom species: **a)** *Cylindrotheca fusiformis*; **b,c)** *Coscinodiscus asteromphalus*; **d,e)** *Thalassiosira pseudonana*.

macromolecules, which have long been speculated to control silica deposition and nanopatterning.[8–10] Only recently have proteins and other organic molecules associated with diatom biosilica been purified to homogeneity and extensively characterized. The current knowledge about the structure and function of these molecules will be summarized in this review.

The cell biology of diatom biosilica formation

The biosilica wall of a diatom cell is constructed in a petri-dish-like fashion being composed of a top half (epitheca) that overlaps the slightly smaller bottom half (hypotheca) (Fig. 2).

Manfred Sumper studied Chemistry at the University of Munich and received his PhD in Biochemistry in 1970 under the supervision of F. Lynen. After a postdoctoral stay at the Max-Planck-Institute of Biophysical Chemistry in Göttingen (M. Eigen) he completed his Habilitation in 1976 at the University of Würzburg (D. Oesterhelt). Since 1978 he has been Full Professor of Biochemistry at the University of Regensburg.

Manfred Sumper

Nils Kröger studied Chemistry at the Universities of Marburg and Regensburg and received his PhD in Biochemistry in 1995 under the supervision of Manfred Sumper. After a postdoctoral stay at the University of Melbourne (Australia) he rejoined the University of Regensburg where he completed his Habilitation in 2001.
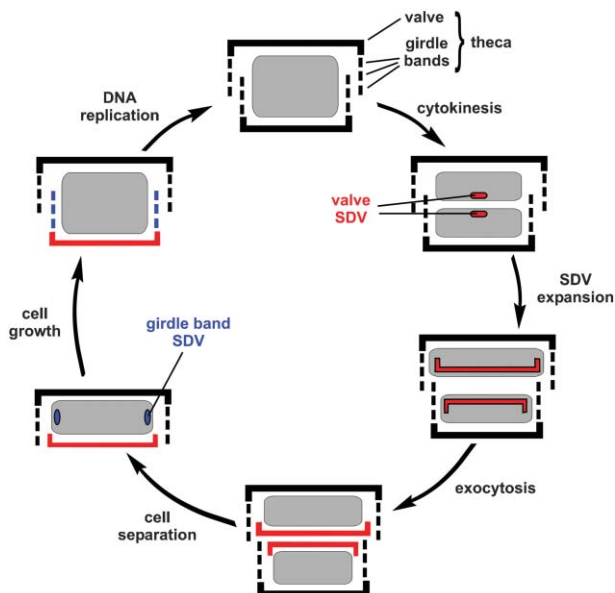
Nils Kröger

Fig. 2 The diatom cell cycle. Schematic cross-sections of the diatom cell are shown. The biosilica cell wall is depicted by black or red bars. The protoplast is shown in grey.

Each theca consists of a valve and several girdle bands, which usually display porous patterns that are far less elaborate than that of the valve. Formation of these biosilica structures takes place in specialized intracellular compartments termed silica deposition vesicles (SDVs).[11] Studies on other silicifying protists have shown that SDVs are not a speciality of diatoms but rather represent general organelles for silica biogenesis.[12]

The immediate precursor for biosilica formation inside the SDV is unknown, yet monosilicic acid $Si(OH)_4$, which occurs in natural habitats in concentrations between 1 and 100 μM, clearly represents the original source for silica formation.[13,14] Monosilicic acid is transported into the diatom cell by specific Na^+-dependent transporter proteins (termed SIT),[15,16] but the mechanism of intracellular storage of soluble silicic acid and its mode of transport to the SDV is not known.[17]

Biogenesis of the diatom cell wall requires two different types of SDVs that are present at different stages of the cell cycle. During cell division each sibling cell produces a valve SDV, which gradually grows as more and more silica becomes deposited. When valve formation is complete, the SDV fuses with the cell membrane depositing the newly formed biosilica structure on the cell surface. Since the biosilica wall is inflexible,

cell growth during interphase is only possible by increasing the distance between epitheca and hypotheca. Therefore, synchronously with cell growth several girdle bands are formed in individual SDVs and are released one after another to the lateral surface of the cell thus preventing the formation of gaps in the cell wall. When the cell volume has reached the required size a new round of cell division commences (Fig. 2).[18]

Organic components of diatom biosilica

From the diatom *C. fusiformis* three families of cell wall proteins (termed frustulins, pleuralins and silaffins) have been isolated and characterized that exhibit novel features.[19–21] In addition, extremely long-chain polyamines (LCPAs) with species-specific chain length distributions have been discovered as constituents of diatom biosilica.[22] Immunoelectron microscopy studies revealed that frustulins and pleuralins are not involved in silica formation because they become associated with the biosilica only after its deposition on the cell surface.[23,24] In contrast, silaffins and polyamines exert a drastic influence on silica formation *in vitro* and thus appear to be directly involved in silica biogenesis (see below).

Silaffins and polyamines are tightly associated with diatom biosilica and can only be solubilized by complete removal of the silica. When *C. fusiformis* biosilica was dissolved using anhydrous HF, three polypeptides, of 17 kDa (silaffin-2), 8 kDa (silaffin-1B) and 4 kDa (silaffin-1A), were solubilized along with a <3.5 kDa non-protein component representing polyamines (Fig. 3a). Protein sequence analysis revealed that silaffin-1A represents a mixture of two very similar peptides (silaffin-$1A_1$, -$1A_2$) which exhibit a high degree of sequence homology to silaffin-1B. Interestingly, the three peptides contained four (silaffin-$1A_1$, -$1A_2$) and six (silaffin-1B) modified lysines (see below). *N*-Terminal sequencing and peptide mapping of silaffin-2 yielded only very limited sequence information, because this protein contains many unidentified amino acid modifications.

Information derived from the N-terminal sequence of silaffin-1B enabled cloning of the corresponding sil1 gene. The N-terminus of the sil1-encoded polypeptide (sil1p) represents a typical signal peptide sequence (amino acids 1 to 19) that is followed by a highly negatively charged domain (amino acids 20 to 107). The remining C-terminal part of sil1p is composed of seven strongly basic repeat units (R1–R7). R1 (amino acids 108 to 140) and R2 (amino acids 141 to 162) contain 33 and 22 amino acids, respectively, whereas the remaining five repeat units (R3 to R7) are shorter, each being composed of 19 amino acid residues (Fig. 3b). Each repeat unit
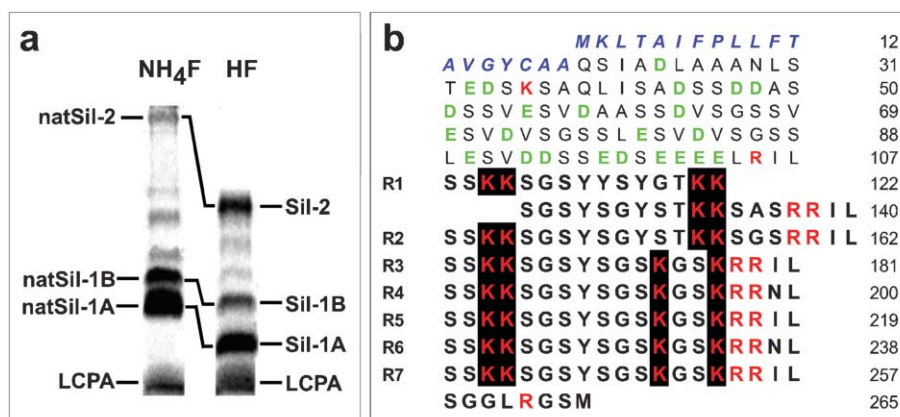

Fig. 3 Silaffins from *C. fusiformis*: **a**) Comparison by Tricine/SDS-PAGE of an ammonium fluoride extract (NH_4F) and a HF extract (HF) from *C. fusiformis* biosilica. **b**) Amino acid sequence of sil1p. The signal peptide is shown in blue italics. Acidic amino acid residues are depicted in bold green and basic amino acid residues in bold red. The silaffin-generating C-terminal domain is shown in bold letters with boxed lysine residues. R1 to R7 indicate the repeating sequence elements within the C-terminal domain. The column of numbers on the right indicates the amino acid positions. Reprinted with permission from *Science* magazine and Wiley-VCH.

contains clusters of lysine and arginine residues that are connected by stretches of hydroxyamino acids (serine, tyrosine) and glycine. Comparing the sil1p sequence with the peptide sequences and mass spectroscopic data of silaffins revealed the following key information about their chemical structures:

(1) The C-terminal part of sil1p (repeat units R1 to R7) becomes proteolytically processed *in vivo* releasing each repeat unit as an individual peptide. Silaffin-1B is derived from repeat unit R1 whereas silaffin-1A represents a mixture of the peptides derived from repeat units R2 to R7. During proteolytical processing, the four C-terminal amino acid residues of each repeat unit (RRIL or RRNL) are cleaved off generating identical 15-mer peptide sequences from R3–R7. Thus, silaffin-1A represents a mixture of the two peptides silaffin-1A$_1$ and silaffin-1A$_2$.

(2) All lysine residues in silaffin-1A$_1$, -1A$_2$ and -1B are modified.

(3) The 'fate' of the acidic N-terminal half of sil1p (amino acids 20–107) is unknown. This peptide could not be identified as a component of the cell wall.

(4) Based on sequence data obtained from silaffin-2 it can be concluded that this protein is not encoded by the sil1 gene.

The extremely high content of hydroxyamino acids in silaffins prompted the speculation that these might be targets for post-translational modifications *in vivo* (*e.g.* glycosylation and phosphorylation). In fact, anhydrous HF, even at 0 °C, is known to cleave exactly these bonds, and thus silaffins may have become deglycosylated and/or dephosphorylated during extraction. Indeed, when silaffin extraction was performed by a gentler method using a slightly acidic, aqueous ammonium fluoride solution the apparent molecular masses of silaffins are substantially larger compared with HF-extracted silaffins. This clearly indicates the existence of HF-labile modifications (Fig. 3a). Since the gentle ammonuim fluoride extraction is likely to preserve the *in vivo* structure of silaffins, the ammonium fluoride-extracted silaffins were termed native silaffins (abbreviated natSil-1A, natSil-1B and natSil-2). Biochemical analysis by peptide mapping, mass spectrometry and ^{31}P NMR revealed the complete chemical structure of natSil-1A$_1$ (Fig. 4a), which is representative for the structures of all sil1p-derived silaffins. NatSil-1A$_1$ contains three different lysine residues representing ε-*N*,*N*-dimethyllysine (position 4), phosphorylated ε-*N*,*N*,*N*-trimethyl-δ-hydroxylysine (position 13) and polyamine-modified lysines (positions 3 and 15). The latter modification is composed of a chain of 6–11 linearly linked

propyleneimine units, in which each N-atom except for the one from the first unit is methylated. The polyamine-modified lysines represent a novel type of amino acid modification that introduces a high number of both positive charges (protonated amino groups) and hydrophobic groups (propylene residues). Additionally, the presence of a total of eight negatively charged phosphate residues confers a unique zwitterionic structure upon natSil-1A$_1$. The zwitterionic character of silaffins is likely to influence their chemical and biological properties strongly (see below).

Only limited information about the chemical structure of natSil-2 has been obtained so far due to the lack of sufficient amino acid sequence information from this protein.[25] NatSil-2 is a phosphoprotein of 40 kDa apparent molecular mass exhibiting a highly complex molecular architecture, because in addition it is glycosylated and sulfated. All lysine modifications identified in silaffin-1 are also present in silaffin-2. Similarly, the amino acid composition is dominated by hydroxyamino acids (serine, threonine, hydroxyproline) and glycine, but the additional presence of significant amounts of methionine and leucine is a distinct feature of silaffin-2. The polypeptide backbone is strongly basic due to the presence of the alkylated lysines, yet the positive charges are overcompensated by the attachment of numerous phosphate, sulfate and glucuronic acid residues conferring a strongly polyanionic character. The phosphorylated amino acids identified are phosphoserine, phosphothreonine and phosphohydroxyproline. Interestingly, natSil-2 represents the first example of a biogenic protein containing phosphohydroxyproline.

Long-chain polyamines exhibit identical apparent molecular masses when extracted by anhydrous HF and aqueous ammonium fluoride, respectively (Fig. 3a), indicating that they carry no HF-sensitive modifications. Polyamines consist of linear chains of N–C-linked propyleneimine units and thus are constructed in the same way as the polyamines found in silaffins. However, the polyamine chain is attached to putrescine or a putrescine derivative rather than to a peptide (Fig. 4b). These polyamines are the longest found in nature, and each diatom species synthesizes a characteristic collection exhibiting variations in chain length and methylation pattern. In most diatom species, long-chain polyamines seem to be at least as abundant as silaffins, and in diatoms of the genus *Coscinodiscus* they appear to be the main organic component associated with biosilica.[26]

Silica chemistry and the structure of silaffins

In the past, a huge amount of knowledge has been accumulated with respect to the complex inorganic chemistry of silicic acid and its polymeric derivatives.[27] These data clearly suggest that the chemistry of silicic acid polycondensation dictates structural adaptations for any biomolecule involved in this process. Non-porous silica nanospheres have been synthesized by controlled hydrolysis of silicon alkoxides in alcohol/NH$_3$ mixtures[28] and the past decade has seen important advances in the ability to fabricate porous solids. Several methodologies have been developed for the synthesis of different silica morphologies summarized in recent reviews.[29–31] By applying this knowledge to the unique structure of the silaffins, a fascinating aspect emerges: nature has designed a molecule that appears to be perfectly adapted to the chemistry of silica formation as briefly outlined. Silicic acid polymerization involves three distinct stages. First, monomeric silicic acid polymerizes by condensation of silanol groups to form dimers, trimers, and cyclic oligomers. Oligosilicic acid species have a strong tendency to further polymerize in such a way that siloxane bond (Si–O–Si) formation is maximized. These early processes create highly branched polysilicic acids as nuclei for silica formation. Second, the nuclei grow to form spherical particles either by continuous polymerization with monomeric and
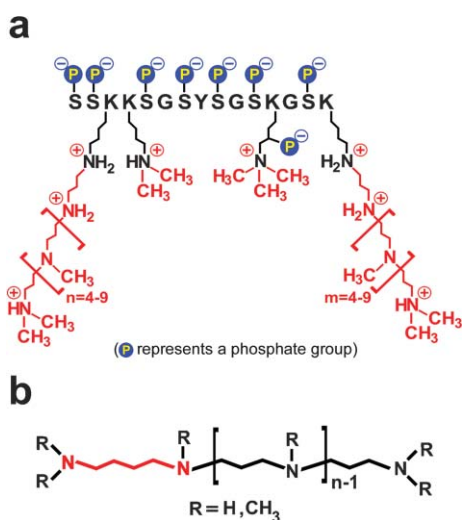
Fig. 4 Chemical structures of silaffins and long-chain polyamines. **a)** Schematic chemical structure of native silaffin-1A$_1$. Post-translational modifications are depicted in colour. The annotation of charges within the molecule is tentative for a solution around pH = 5. **b)** General, schematic chemical structure of long-chain polyamines. The putrescine moiety is shown in red.

oligomeric silicic acids or by fusion of particles. Finally, the silica nanospheres can form a three-dimensional network forming branched particle chains that are cross-linked by siloxane bonds. As a consequence, the molecular masses of the polysilicic acids increase, the sol becomes more and more viscous and ultimately hardens as a gel (gelling). Alternatively, the particles precipitate by flocculation, a process that intimately connects and close-packs silica spheres producing hard silica as it is found in the diatom cell wall. The structural elements of silaffins are likely to be involved in each of these three stages, thereby accelerating the formation of hard silica by several orders of magnitude. More than 40 years ago, quaternary ammonium ions were recognized as structure-directing agents in the synthesis of zeolite molecular sieves.[32] The tetramethylammonium cation favours the formation of symmetric oligosilicate anions like the cubic octamer $Si_8O_{20}^{8-}$ and this control of silicate speciation influences the nucleation phase of silica formation.[33] Owing to their unique ε-N,N,N-trimethyl-δ-hydroxylysine residue, silaffins may exert a similar control. Polyamines were shown to catalyse the polycondensation of silanol groups[34] and in addition are known to act as an efficient flocculation agent.[27] The polyamine side chains of silaffins are likely to have exactly these functions *in vivo* because diatom biosilica formation is very rapid and corresponds to silica flocculation rather than gelling. This is strongly supported by numerous observations in different diatom species demonstrating that silica is initially laid down as tightly associated spheres of 10–100 nm in diameter.[35–38] There have also been reports of the presence of fibrillar silica strands within developing SDVs.[39,40] Such fibrils might actually be composed of linear rows of partially fused silica spheres.

Recently, an additional type of modification, a high degree of phosphorylation of silaffins, has been shown to be essential for silica nanosphere formation *in vitro*. The functional role of phosphorylation will be discussed below.

Silica formation by natSil-1A

When native silaffin-1A is added to a slightly acidic silicic acid solution (pH 5.5), silica is rapidly precipitated within only a few minutes,[41] whereas in the absence of silaffins the solution very slowly hardens as a gel. Thus, natSil-1A highly accelerates the polycondensation of silicic acid and acts as a flocculating agent. The following data demonstrate that this activity is critically dependent upon all types of post-translational modifications:

(1) Dephosphorylated natSil-1A is unable to induce silica formation *in vitro* unless a sufficient concentration of inorganic phosphate is included in the assay.[41]

(2) In the presence of inorganic phosphate, silaffin-1A exhibits silica formation activity over a wide pH range down to pH 4.2. In contrast, the synthetic silaffin peptide pR5, which does not carry any amino acid modifications, exhibits silica formation activity only in the neutral and alkaline pH range.[21] Since the SDV of diatoms is an acidic compartment,[42] it can be concluded that the lysine modifications are essential for silica formation activity under physiological conditions.

Insight into the mechanism of natSil-1A-mediated silica formation was gained by ^{31}P NMR spectroscopy, which demonstrated that natSil-1A is not monomeric in solution but forms supramolecular assemblies containing about 700 peptide molecules. The self-assembly is mediated by intermolecular interactions between the numerous positively and negatively charged groups of the zwitterionic molecules.[41] We suggest that this self-assembly is a prerequisite for silica formation because such assemblies may provide a template for silicic acid polycondensation. Dephosphorylation inhibits self-assembly because natSil-1A is then converted to a highly positively charged molecule, being no longer able to form supramolecular assemblies by electrostatic interactions. The addition of

phosphate anions restores the silica precipitation activity, presumably because phosphate anions can serve as ionic cross-linkers promoting the aggregation.

Information regarding the function of the polyamine moieties of natSil-1A was obtained by the discovery that long-chain polyamines alone exhibit silica formation activity in the presence of inorganic phosphate or other polyvalent anions.[22] The kinetics and pH dependence of polyamine-induced silica formation are similar to the properties of natSil-1A, thus indicating that the interaction of natSil-1A with silicic acid molecules is mediated *via* the polyamine moieties. The underlying mechanism was further studied by investigating the polyamine-mediated silica formation.

Silica formation by long-chain polyamines

Recently, the function of phosphate anions in the polyamine-directed formation of silica nanospheres using the polyamines extracted from the cell wall of *Stephanopyxis turris*[43] or synthetic polyallylamine[44] was studied. The *S. turris* poly-amines consist of 15 to 21 *N*-methyl-propyleneimine repeated units attached to putrescine. These polyamines were able to precipitate silica nanospheres from a silicic acid solution after a few minutes, even under acidic conditions (Fig. 5a, blue line). However, this precipitation was strictly dependent upon the presence of multivalent anions like phosphate. In the presence
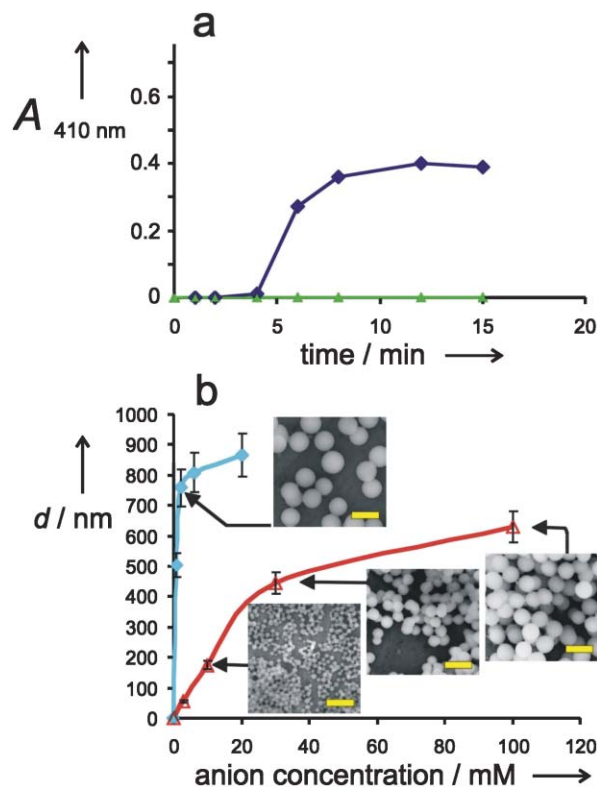
Fig. 5 Characteristics of silica fabrication catalyzed by the polyamine/phosphate system. **a**) Kinetics of silica precipitation. The incubation mixture contained 30 mM sodium phosphate, pH 5.5, 0.2 mM polyamine, and 40 mM mono-/di-silicic acid. Precipitated silica was dissolved in 2 M NaOH (5 min at 90 °C) and quantified by the molybdate method. Blue line, all components were mixed at $t = 0$ min. Green line, phosphate was replaced by 30 mM sodium acetate, pH 5.5. **b**) Silica nanosphere diameters as a function of the multivalent anion concentration. Silica fabrication was performed in a 30 mM sodium acetate buffer, pH 5.5 as in (**a**) with increasing concentrations of multivalent anions. The reaction was allowed to proceed for 12 min. The resulting nanospheres were collected by centrifugation and analyzed by SEM. Response to orthophosphate and pyrophosphate is shown by the red and the blue lines, respectively. Insets, SEM micrographs of the corresponding precipitates. Scale bars, 1 μm. Reprinted with permission from Wiley-VCH.

of acetate anions only (the buffer system), no precipitate at all was formed (Fig. 5a, green line). Interestingly, the particle size of the silica nanospheres is strictly controlled by the concentration of phosphate anions (Fig. 5b, red line). Defined particle diameters between 50 and 700 nm could be obtained and the resulting size distributions were close to monodisperse. Replacement of orthophosphate by pyrophosphate, an anion with a higher negative charge, exhibited a drastic effect. Control of nanosphere size distribution was exerted at anion concentrations nearly two orders of magnitude lower and the maximum sphere diameter was increased to about 1000 nm (Fig. 5b, blue line). Other multivalent anions (e.g. citrate, sulfate) are capable of producing silica precipitates as well, whereas monovalent anions such as chloride or acetate failed to do so.

Long-chain polyamines behave like amphiphilic substances because they are extractable from an aqueous solution by chloroform/methanol (3:2 by volume). Possibly, these polyamines form aggregates in aqueous solution with positively charged surfaces. If so, increasing concentrations of multivalent anions should promote higher order assemblies of aggregates and therefore produce emulsion droplets of increasing size. Phosphate is likely to act as a cross-linking agent as it is able to establish hydrogen bonds as well as electrostatic interactions (charge-stabilized hydrogen bonds). These assumptions could be confirmed by NMR and dynamic light scattering techniques using the synthetic polyallylamine/phosphate system.[44] Microscopic phase separation turned out to be essential for the polyamine-induced silica precipitation. Mono-, oligo- or poly-silicic acid molecules may be adsorbed on and/or dissolved in the polyamine microdroplets, thereby forming a coacervate (formation of a 'liquid precipitate') which finally hardens by silica formation. This mechanism is able to explain the observed correlation between phosphate anion concentration and the size of the resulting silica nanospheres.

A model for morphogenesis of biosilica nanopatterns by polyamines

Diatoms of the genus *Coscinodiscus* exhibit extraordinarily intricate silica patterns including fine structures in the 30 to 50 nm range (see Fig. 1c). The valve structure can be interpreted as being composed of a hierarchy of self-similar hexagonal silica structures producing the complex but highly symmetric valve patterning. Surprisingly, HF-extracts from these diatoms exhibited only long-chain polyamines. These observations stimulated a model of pattern formation that is exclusively based on the physicochemical properties of polyamines. Based on the assumption that polyamines phase separate within the SDV to form emulsions of microdroplets, it is possible to explain the observed stages of cell wall biogenesis in *Coscinodiscus*.[26] In a close-packed arrangement the microdroplets would form a hexagonal monolayer within the flat SDV. The aqueous interface between polyamine droplets contains the as yet unknown silica precursors and promotes silica formation (Fig. 6a). Thus the precipitating silica necessarily creates a honeycomb-like framework. Silica formation consumes a defined fraction of the polyamine population by co-precipitation.[21,22] This fact is assumed to cause a dispersion of the original organic droplets segregating smaller droplets (Fig. 6b). Guided by the newly created water/polyamine interfaces, silica continues to precipitate, thereby consuming another fraction of the polyamine population. This in turn causes the remaining part of the original organic droplet to break up into a maximum number of smaller droplets, again creating new interfaces for silica deposition (Fig. 6c). Iteration of this simple mechanism would create the nanopattern observed in *Coscinodiscus* valves.

Including the most recent experimental results in this model, polyamine phase separation requires a polyanionic component, and the original size of microdroplets might be controlled by a defined polyamine/multivalent anion ratio as it was demonstrated *in vitro*. Probably, an as yet unidentified phosphorylated protein in *Coscinodiscus* represents the anionic partner required for polyamine phase separation. In summary, polyamines (as well as silaffins representing peptide-bound polyamines) together with a polyanionic partner are assumed to undergo a phase separation process in the SDV that creates a pattern of areas promoting silica formation.

A number of diatom genera exhibit less symmetric biosilica nanopatterns (see Fig. 1e), which demands additional components that break up the inherently hexagonal arrangement of the proposed polyamine microdroplets. This may be achieved by the formation of an organic matrix composed of more complex mixtures of polyamines and polyanionic silaffins (see below).

Control of silica morphogenesis by silaffins

The model studies with polyamines are likely to be also relevant for the function of silaffins. However, owing to the complex structures of silaffins, their exact mode of action in silica formation remains to be established. Some recent observations regarding the behaviour of silaffins in silica morphogenesis are summarized in the following.

Silica morphogenesis by supramolecular natSil-1A assemblies *in vitro* was investigated by SEM in a time-resolved manner
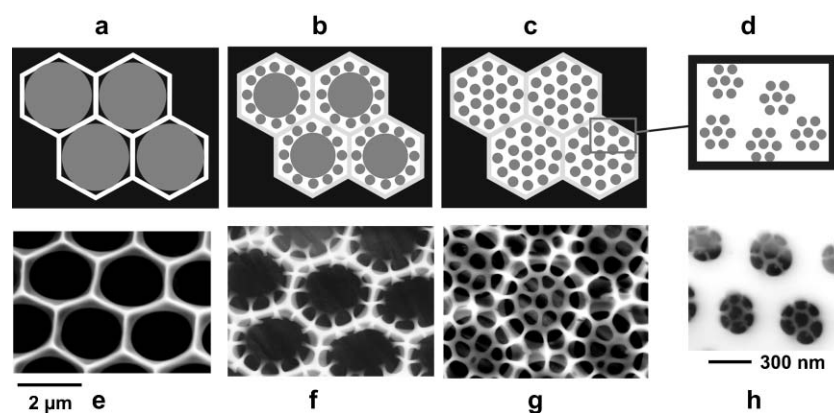

Fig. 6 Schematic drawing of the templating mechanism by the phase separation model (**a–d**) and comparison with different stages of the cell wall biogenesis of *C. wailesii* (**e–h**). **a**) The monolayer of polyamine-containing droplets in close-packed arrangement within the silica deposition vesicle guides silica deposition. **b,c**) Consecutive segregations of smaller (about 300 nm) droplets open new routes for silica precipitation. **d**) Dispersion of 300 nm droplets into 50 nm droplets guides the final stage of silica deposition. Silica precipitation only occurs within the water phase (white areas). The repeated phase separations produce a hierarchy of self-similar patterns. **e–h**) Scanning electron micrographs of valves *in statu nascendi* at the corresponding stages of development. Reprinted with permission from *Science* magazine.
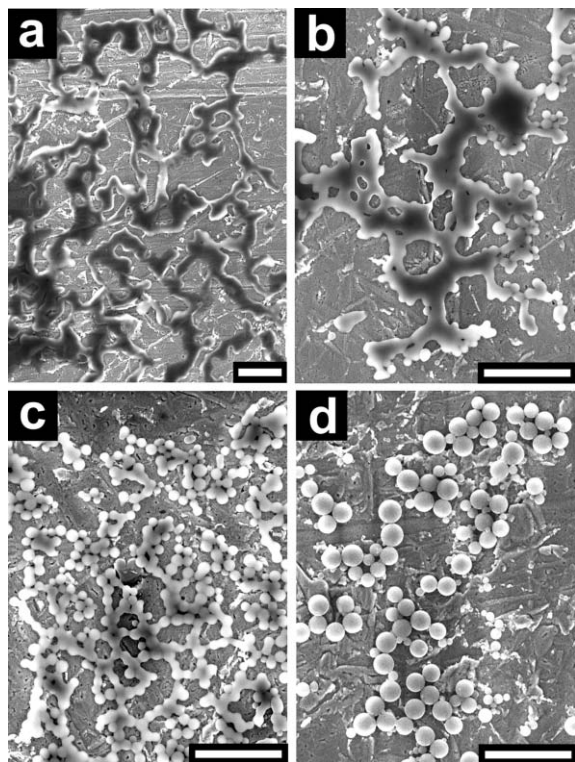
Fig. 7 Analysis of natSil-1A-induced silica morphogenesis *in vitro*. SEM images of silica structures formed 3.5 min (**a**), 4.5 min (**b**), 5 min (**c**) and 8 min (**d**) after the addition of natSil-1A to a 100 mM monosilicic acid solution buffered at pH 5.5 (50 mM sodium acetate). Scale bars, 2 μm. Reprinted with permission from *Science* magazine.

(Fig. 7). About 3 min after the addition of silicic acid the first silica structures were discernible and appeared (after an unavoidable drying step) as extended flat networks of irregularly shaped, branched bands (Fig. 7a). These networks represent a silicified silaffin phase that contains both silica and natSil-1A, as demonstrated by elemental analysis using EDXA. This early phase appears to be elastic since a few minutes later it becomes transformed into large spherical particles (diameter 400–700 nm) that still contain both silica and natSil-1A (Fig. 7b–d). These spheres, which are the end products of this amazing silica morphogenesis process, are certainly too large to be of any biological relevance since diatom biosilica is composed of particles that are only 10–100 nm in size.[35–38] However, the apparently elastic silaffin–silica phase observed at the early stages may represent the mouldable biosilica material used to form the silica elements of *C. fusiformis*, which do not exhibit any patterning by nanosized pores.

An unexpected behaviour was found for native silaffin-2. Surprisingly, this large silaffin species is incapable of forming silica *in vitro* (Fig. 8a, red line) although it contains the polyamine-modified lysines that confer silica formation activity on all silaffin-1 species. It has been shown that the lack of silica precipitation activity in natSil-2 is caused by its anionic modifications (sulfation and glycosylation) which auto-inhibit the silica formation activities of the polyamine moieties.[25] However, when combined with long-chain polyamines, rapid silica precipitation occurs under conditions at which polyamines alone are unable to form silica (Fig. 8a, green line). Most probably, native silaffin-2 acts as the polyanion required for polyamine phase separation. At higher concentrations, however, native silaffin-2 exerted an inhibitory effect on polyamine-induced silica formation (Fig. 8a, black line). Owing to these pleiotropic effects, native silaffin-2 may be regarded as a regulator of silica formation.

Although natSil-2 lacks intrinsic silica formation activity it is able to influence silica morphogenesis. This was demonstrated
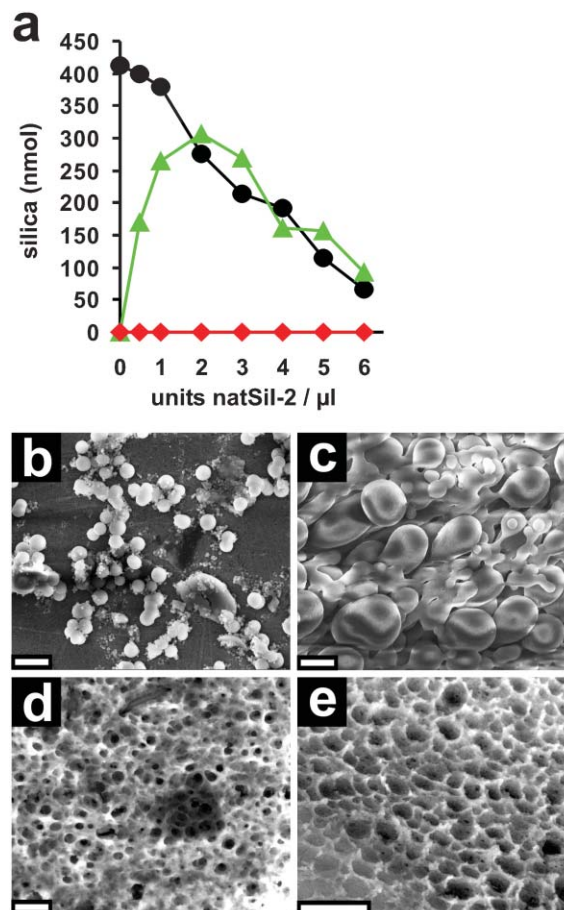

Fig. 8 Influence of natSil-2 on silica formation. **a**) Silica precipitation experiments were performed with natSil-2 only (red) and with mixtures of natSil-2 and 0.6 μg μl^{-1} LCPA (green) or 0.3 mM natSil-1A (black), respectively (1 unit is defined as 1 nmol natSil-2 bound phosphate). **b–d**) SEM analysis of silica precipitates formed by mixtures of natSil-1A and natSil-2 (scale bars, 2 μm): **b**) 0.5 units μl^{-1} natSil-2, 0.3 mM natSil-1A; **c**) 5.0 units μl^{-1} natSil-2, 0.3 mM natSil-1A; **d**) 2.0 units μl^{-1} natSil-2, 0.3 mM natSil-1A; **e**) 1.6 units μl^{-1} natSil-2, 0.2 mM natSil-1A. Reprinted with permission from the National Academy of Sciences, USA.

by SEM analysis of the silica precipitates formed by mixtures of natSil-2 and natSil-1A or polyamines, respectively. Fig. 8b–e show the silica structures that were produced at pH 5.5 by different native silaffin-1A/-2 ratios 10 min after the addition of silicic acid. At high and low ratios, polydisperse silica spheres (diameters 100–1000 nm; Fig. 8b) and large interconnected spherical or pear-shaped silica particles (Fig. 8c), respectively, were obtained. At intermediate ratios, the formation of silica particles became suppressed and porous silica blocks were formed (Fig. 8d,e). Remarkably, the pore sizes were in the range of 100–1000 nm, which matches the characteristic size range of diatom biosilica nanopores. Similar structures could be generated using appropriate mixtures of polyamines and native silaffin-2. Based on these *in vitro* results, the lack of any nanopore patterning in *C. fusiformis* biosilica may be explained by the presence of extremes of silaffin-1/-2 ratios within the SDV. The interesting conclusion, however, that can be drawn from these observations is that native silaffins possess the inherent ability to guide nanopattern formation if mixed in the appropriate ratios.

When native silaffin-1 and -2 are combined, a dense, pelletable silaffin-phase (silaffin matrix) was created that could be readily separated from the aqueous phase by centrifugation.[25] It is likely that silicic acids become concentrated within this matrix by interaction with the long-chain polyamine moieties, thus increasing the rate of condensation. Taken together, only two types of organic biomolecules appear to be sufficient to

produce biologically relevant silica structures: polycationic molecules, which exhibit silica-forming activity, and polyanionic components, which allow the self-assembly of the system and possibly act in addition as regulators.

Biomimetic synthesis of silica-based devices

Since the discovery of silaffins and long-chain polyamines and their remarkable effects on silica formation, research has been undertaken to apply this knowledge for biomimetic synthesis of nanostructured silica-based materials.[45–48] Very promising results towards this direction were obtained by Stone and co-workers,[49] who have used the synthetic silaffin-1-derived peptide R5 to produce silica materials with potential technological applications. This peptide lacks all amino acid modifications characteristic for native silaffins but exhibits silica precipitation activity under ambient conditions when added to a silicic acid solution at $\geqslant$ pH 7.[21] To produce an ordered hybrid organic/inorganic nanostructure, peptide R5 was included in a two-photon-induced polymerization process that creates an undulated organic polymer exhibiting a periodicity of 1.33 μm. When the polymer was exposed under ambient conditions to a silicic acid solution at pH 8, an ordered array of silica nanospheres (diameters 451 $\pm$ 81 nm) was deposited within 10 min exclusively in the troughs of the polymer. This effect is due to the accumulation of R5 peptides in the troughs rather than the crests of the developing polymer. Interestingly, the silica–organic polymer exhibited an almost fifty-fold increase in diffraction efficiency over a comparable polymer without silica, which is crucially important to the employment of this hybrid material for fabrication of photonic devices.[49] Very recently, R5-mediated silica formation was also used to encapsulate enzymes in a silica matrix without any loss of enzyme activity.[50] Within the silica matrix, the enzyme butyrylcholinesterase was significantly more stable than in solution, and the mechanical properties of this material allowed rapid turnover rates in a flow-through reactor. Since silaffin peptides are able to control silica morphology and the polyamine/phosphate system can be used to produce silica nanospheres with predetermined diameters, the production of structurally tailored catalyst matrices should be feasible.

Given these encouraging examples, it can be expected that forthcoming information about the molecules and mechanisms of biosilica morphogenesis in diatoms will pave the way for the fabrication of nanostructured silica-based materials with novel properties.

Acknowledgements

References

1   H. A. Lowenstam and S. Weiner, *On Biomineralization*, Oxford University Press, Oxford, 1989.
2   E. Epstein, *Ann. Rev. Plant Physiol. Plant Mol. Biol.*, 1999, **50**, 641–664.
3   A. L. Samuels, A. D. M. Glass, J. G. Menzies and D. L. Ehret, *Physiol. Mol. Plant Pathol.*, 1994, **44**, 237–242.
4   K. Schwarz, *Proc. Natl. Acad. Sci. USA*, 1973, **70**, 1608–1612.
5   E. M. Carlisle, in Silicon and Siliceous Structures in Biological Systems, T. L. Simpson and B. E. Volcani, ed., Springer, New York, 1981, p. 69.
6   S. Mann and G. Ozin, *Nature*, 1996, **382**, 313–318.
7   J. Parkinson and R. Gordon, *Trends Biotechnol.*, 1999, **17**, 190–196.
8   T. Nakajiama and B. E. Volcani, *Science*, 1969, **164**, 1400–1406.
9   R. Hecky, K. Mopper, P. Kilham and T. Degens, *Mar. Biol.*, 1973, **19**, 323–331.
10 D. Swift and A. Wheeler, *J. Phycol.*, 1992, **28**, 202–209.
11 R. W. Drum and H. S. Pankratz, *J. Ultrastruct. Res.*, 1964, **10**, 217–223.
12 T. L. Simpson and B. E. Volcani, *Silicon and Siliceous Structures in Biological Systems*, Springer, New York, 1981.
13 P. Tréguer, D. M. Nelson, A. J. van Bennekom, D. J. DeMaster, A. Leynaert and B. Quéguiner, *Science*, 1995, **268**, 375–379.
14 Y. Del Amo and M. A. Brzezinski, *J. Phycol.*, 1999, **35**, 1162–1170.
15 M. Hildebrand, B. E. Volcani, W. Gassmann and J. I. Schroeder, *Nature*, 1997, **385**, 688–689.
16 M. Hildebrand, K. Dahlin and B. E. Volcani, *Mol. Gen. Genet.*, 1998, **260**, 480–486.
17 V. Martin-Jézéquel, M. Hildebrand and M. A. Brzezinski, *J. Phycol.*, 2000, **36**, 821–840.
18 J. Pickett-Heaps, A. M. Schmid and L. A. Edgar, in *Progress in Phycological Research: Vol. 7*, F. E. Round and D. J. Chapman, ed., Biopress, Bristol, 1990, pp. 1–168.
19 N. Kröger, C. Bergsdorf and M. Sumper, *EMBO J.*, 1994, **13**, 4676–4683.
20 N. Kröger, G. Lehmann, R. Rachel and M. Sumper, *Eur. J. Biochem.*, 1997, **250**, 99–105.
21 N. Kröger, R. Deutzmann and M. Sumper, *Science*, 1999, **286**, 1129–1132.
22 N. Kröger, R. Deutzmann, C. Bergsdorf and M. Sumper, *Proc. Natl. Acad. Sci. USA*, 2000, **97**, 14133–14138.
23 W. H. van de Poll, E. G. Vrieling and W. W. C. Gieskes, *J. Phycol.*, 1999, **35**, 1044–1053.
24 N. Kröger and R. Wetherbee, *Protist*, 2000, **151**, 263–273.
25 N. Poulsen, M. Sumper and N. Kröger, *Proc. Natl. Acad. Sci. USA*, 2003, **100**, 12 075–12 080.
26 M. Sumper, *Science*, 2002, **295**, 2430–2433.
27 R. K. Iler, *The Chemistry of Silica*, Wiley, New York, 1979.
28 J. Stöber, A. Fink and E. Bohn, *J. Colloid Interface Sci.*, 1968, **26**, 62–69.
29 S. Mann, *Angew. Chem., Int. Ed.*, 2000, **39**, 3392–3406.
30 M. E. Davis, *Nature*, 2002, **417**, 813–821.
31 K. J. van Bommel, A. Friggeri and S. Shinkai, *Angew. Chem., Int. Ed.*, 2003, **42**, 980–999.
32 R. M. Barrer and P. J. Denny, *J. Chem. Soc.*, 1961, 971–982.
33 D. Hoebbel, G. Garzo, G. Engelhardt, R. Ebert, E. Lippmaa and M. Alla, *Z. Anorg. Allg. Chem.*, 1980, **465**, 15–33.
34 T. Mizutani, H. Nagase, N. Fujiwara and H. Ogoshi, *Bull. Chem. Soc. Jpn.*, 1998, **71**, 2017–2022.
35 M. L. Chiappino and B. E. Volcani, *Protoplasma*, 1977, **93**, 205–221.
36 A. M. M. Schmid and D. Schulz, *Protoplasma*, 1979, **100**, 267–288.
37 S. A. Crawford, M. J. Higgins, P. Mulvaney and R. Wetherbee, *J. Phycol.*, 2001, **37**, 543–554.
38 F. Noll, M. Sumper and N. Hampp, *Nano Lett.*, 2002, **2**, 91–95.
39 J. Pickett-Heaps, D. Tippit and J. Andreozzi, *Biol. Cell*, 1979, **35**, 199–206.
40 C. W. Li and B. E. Volcani, *Philos. Trans. R. Soc. London, Ser. B*, 1984, **304**, 519–528.
41 N. Kröger, S. Lorenz, E. Brunner and M. Sumper, *Science*, 2002, **298**, 584–586.
42 E. G. Vrieling, W. W. C. Gieskes and T. P. M. Beelen, *J. Phycol.*, 1999, **35**, 548–559.
43 M. Sumper, S. Lorenz and E. Brunner, *Angew. Chem., Int. Ed.*, 2003, **42**, 5192–5195.
44 E. Brunner, K. Lutz and M. Sumper, *Phys. Chem. Chem. Phys.*, 2004, **6**, 854–857.
45 S. V. Patwardhan and S. J. Clarson, *J. Inorg. Organomet. Polym.*, 2002, **12**, 109–115.
46 R. R. Naik, P. W. Whitlock, F. Rodriguez, L. L. Brott, D. D. Glawe, S. J. Clarson and M. O. Stone, *Chem. Commun.*, 2003, 238–239.
47 S. V. Patwardhan, N. Mukherjee, M. Steinitz-Kannan and S. J. Clarson, *Chem. Commun.*, 2003, 1122–1123.
48 E. G. Vrieling, S. Hazelaar, W. W. C. Gieskes, Q. Sun, T. P. M. Beelen and R. A. van Santen, in *Prog. Mol. Subcell. Biol.*, W. E. G. Müller, ed., Springer, Berlin, Heidelberg, 2003, **33**, pp. 301–334.
49 L. L. Brott, R. R. Naik, D. J. Pikas, S. M. Kirkpatrick, D. W. Tomlin, P. W. Whitlock, S. J. Clarson and M. O. Stone, *Nature*, 2001, **413**, 291–293.
50 H. R. Luckarift, J. C. Spain, R. R. Naik and M. O. Stone, *Nat. Biotechnol.*, 2004, **22**, 211–213.